

Fast Anion-Conduction in Oxynitrides: Oxygen and Nitrogen Transport in (Y, Zr)-(O, N)

Martin Kilo,^{*,1} Marcela Andrea Taylor,^{1,4} Günter Borchardt,¹ Ines Kaiser-Bischoff,² Hans Boysen,² Christoph Rödel³ and Martin Lerch³

¹ IMET, TU Clausthal, Robert-Koch-Str. 42, D-38678 Clausthal-Zellerfeld, Germany

² Department für Geo- und Umweltwissenschaften, Sektion Kristallographie, Ludwig-Maximilian-Universität München, Theresienstr. 41, D-80333 München, Germany

³ TU Berlin, Institut für Chemie, Straße des 17. Juni 135, D-10623 Berlin, Germany

⁴ On leave from Dto. de Física, Fac. Cs. Ex. - U.N.L.P. and IFLP - CONICET, Argentina

E-Mail: martin.kilo@tu-clausthal.de

*Presented on the Bunsen Colloquium: Diffusion and Reactions in Advanced Materials
September 27th – 28th, 2007, Clausthal-Zellerfeld, Germany*

Keywords: zirconium oxynitride, nitrogen diffusion, oxygen diffusion, neutron scattering

Abstract. Cation doped zirconium oxynitrides (for example zirconium oxide doped with yttrium oxide and nitrogen, 'YZrON'), having a fluorite-based structure, are suggested to have fairly high nitrogen diffusivity, besides their high oxygen mobility. In the present work, the tracer-diffusion of nitrogen and oxygen was measured in single crystalline 'YZrON'. Results are compared to the migration pathways and migration enthalpies of nitrogen and oxygen ions as determined by elastic neutron diffraction studies. Excellent agreement of the measured activation enthalpies of nitrogen diffusion (about 2 eV) and oxygen diffusion (about 1 eV) determined by the two methods is found.

1 Introduction

It is widely known that cubic stabilised zirconia can be obtained by the addition of lower valent oxides like yttria or calcia to zirconium oxide leading to YSZ or CSZ, respectively [1, 2]. These materials exhibit a very high ionic conductivity due to their inherently high concentration of oxygen vacancies, which are formed because of the addition of the dopant oxides via the following reaction (eqn. 1):



An alternate way to increase the concentration of vacancies in the anion lattice is the incorporation of higher valent anions in the stabilised zirconia materials leading to metal-zirconium (yttrium) oxynitrides, e.g. 'YZrON' [3]. It was recently shown that the incorporation of a few mol-% nitrogen into YSZ increases the ionic conductivity by a factor of three

[4], more than would be expected by using simple defect chemistry assuming that the increase is simply given by an enhanced number of anion vacancies via equation 2.



It is suspected that the increased ionic conductivity might be at least partially due to an enhanced transport of nitrogen. Furthermore, zirconium oxynitride has a very high mechanical stability making it also a very attractive material for structural applications [5]. Unfortunately, the ionic conductivity seems to decrease with time [4] which was attributed to an effect of ordering: Doped zirconium oxynitrides show a strong tendency to form long-range ordered rhombohedral phases (similar to the β -phase in the system $\text{ZrO}_2\text{-Sc}_2\text{O}_3$, [6]), whose detailed structures have been solved only recently [7, 8].

Of particular interest is the question of the coordination of the two different cations (Y^{3+} , Zr^{4+}) with the three different species in the anion sublattice (O^{2-} , N^{3-} , anion vacancies $\text{V}_\text{O}^{2\bullet}$). In principle, these 5 species could associate to form partly ordered systems. This association could be due to the ionic size or due to the ionic charge. For nitrogen-free zirconia stabilized only with cations, the both effects can play a role [9]. However, it is not evident that there is a preferential ordering between species on the cation and anion sites, and — if there is an ordering effect — whether charge effects or size effects are predominating. Recent studies of ionic conductivity suggest that both effects play a role, depending on temperature and type and amount of dopants [10].

2 Experimental

'YZrON' single crystals of the nominal composition $\text{Zr}_{0.83}\text{Y}_{0.17}\text{O}_{1.72}\text{N}_{0.14}$ were obtained by annealing yttria-stabilised zirconia (YSZ) single crystals in nitrogen at 2000 K. The amount of nitrogen incorporated into the material was determined by hot gas extraction.

Layers of 'YZrON' enriched with the stable isotopes ^{15}N and ^{18}O were prepared by implantation. The isotopes were implanted down to 40-50 nm sample depth with an ion dose of $3 \times 10^{16} \text{ cm}^{-2}$. The nitrogen and oxygen tracer-diffusion was investigated in vacuum ($< 10^{-7}$ mbar) at temperatures between 650 and 1000 K and the depth distributions of the nitrogen and oxygen isotopes were analysed using SIMS (SIMS: Secondary Ion Mass Spectroscopy; used machines: Cameca ims 3f, VG SIMSlab). Further details can be found elsewhere [11].

Single crystal neutron diffraction was performed on 'YZrON' and YSZ containing different amounts of nitrogen and oxygen at the instrument D9 of ILL Grenoble, France, at room temperature and 800 °C, respectively. A major advantage of neutron diffraction as compared to the more common X-ray diffraction techniques is that it is much more sensitive for lighter elements, here, in particular, the anions O^{2-} and N^{3-} . Moreover, O and N can be distinguished easily, which is practically impossible with X-rays. From an analysis of the intensities of the Bragg peaks, it is possible to get information on the average defect structures via an analysis of the Debye-Waller factors. From these, probability density functions (PDF), *i.e.*, the average distribution of the ions, can be calculated, giving information, *e.g.*, on the migration pathways. By employing Boltzmann statistics 3-dimensional effective single particle potentials (in which the ions move) can be extracted containing the potential barriers to migration. The latter may be compared to the diffusion enthalpies obtained by other methods. It should be noted that these enthalpies are only related to migration, *i.e.*, they do not contain any possible additional enthalpy for the formation of defects [12]. Furthermore, from an analysis of the diffuse scattering information about the short-range order and defect correlations can be obtained [13].

3. Results and Discussion

3.1 Preparation

Zirconium oxide, stabilized with yttria, can be nitrided to a maximum level of ca. 3 wt%, corresponding to more than 10 mol% on the anion sublattice. The maximum amount of nitrogen taken up by YSZ is decreasing when increasing the yttrium level. The nitrided zirconias were of the cubic fluorite type, as confirmed by XRD.

For the tracer diffusion experiments, YSZ samples containing 9.5 mol% of yttria were nitrided to a level of 1.6 wt% nitrogen. For the neutron diffraction experiments, the following three sample compositions were investigated: (A) $Zr_{0.83}Y_{0.17}O_{1.68}N_{0.16}$, (B) $Zr_{0.74}Y_{0.26}O_{1.87}$ and (C) $Zr_{0.96}Y_{0.04}O_{1.64}N_{0.22}$. Sample (A) is almost identical to the sample investigated by tracer diffusion.

3.2 Tracer Diffusion

Tracer diffusivities D were determined by fitting appropriate solutions of Fick's second law [14] to the tracer isotope concentration profile. Eqn. 3 was used to describe nitrogen diffusion in the doped 'YZrON' (see also a typical depth profile in Fig. 1):

$$c(x,t) = \frac{I(^{15}\text{N})}{I(^{14}\text{N}) + I(^{15}\text{N})} = \frac{Q}{\left(2\pi(\Delta R_p^2 + 2Dt)\right)^{\frac{1}{2}}} \exp\left(-\frac{(x - R_p)^2}{2(\Delta R_p^2 + 2Dt)}\right) \quad (3)$$

Here, Q is the implanted dose of ^{15}N , $I(^{15}\text{N})$ and $I(^{14}\text{N})$ are the measured SIMS isotope or cluster intensities, R_p is the implantation depth and ΔR_p is the width of the initial Gauss profile. For the data evaluation of the annealed samples, the experimental obtained values of ΔR_p and R_p in the as-implanted samples were used, which were slightly higher than the value expected from the SRIM [15] simulations ($R_{p,\text{SRIM}} = 51$ nm; $\Delta R_{p,\text{SRIM}} = 46$ nm; the SRIM calculations were performed assuming amorphous crystals).

When plotting $\ln D(^{15}\text{N})$ vs. $1/T$, one gets a constant slope leading to an activation enthalpy of about 2.2 eV and a preexponential factor of 0.8 cm^2/s (Fig. 2 and eqn. (4)).

$$D(^{15}\text{N}) = 0.8 \cdot e^{-2.2 \text{ eV}/kT} \text{ cm}^2 \text{ s}^{-1} \quad (4)$$

The error in ΔH is ± 0.2 eV, while the error in D_0 corresponds to $\ln D_0 = -0.22 \pm 2.1$. In the case of the oxygen diffusion, we obtained an activation enthalpy of 0.95 eV for bulk self-diffusion, roughly half of the value observed for nitrogen diffusion. The pre-exponential factor was $10^{-7} \text{ cm}^2 \text{ s}^{-1}$ for oxygen self-diffusion (eqn. (5)).

$$D(^{18}\text{O}) = 10^{-7} \cdot e^{-0.95 \text{ eV}/kT} \text{ cm}^2 \text{ s}^{-1} \quad (5)$$

Arrhenius plots of the nitrogen and oxygen self-diffusion, given in Figs. 2 and 3, show that the diffusion of nitrogen and oxygen are nearly the same at a temperature around 1000 K. Moreover, the diffusivities obtained here, as compared with the oxygen and cation diffusion in YSZ without nitrogen, show that the nitrogen diffusion is slower than the oxygen diffusion by four orders of magnitude (ref. [14] and similar values in ref. [16]), but still many orders of magnitude faster than cation diffusion in stabilized zirconias [11,17].

The activation entropy ΔS of diffusion, as derived from the pre-exponential factor of 0.8 cm^2/s , was calculated according to [14]:

$$\Delta S / k_B = \ln \frac{6D_0}{a^2 f v_0} \quad (6)$$

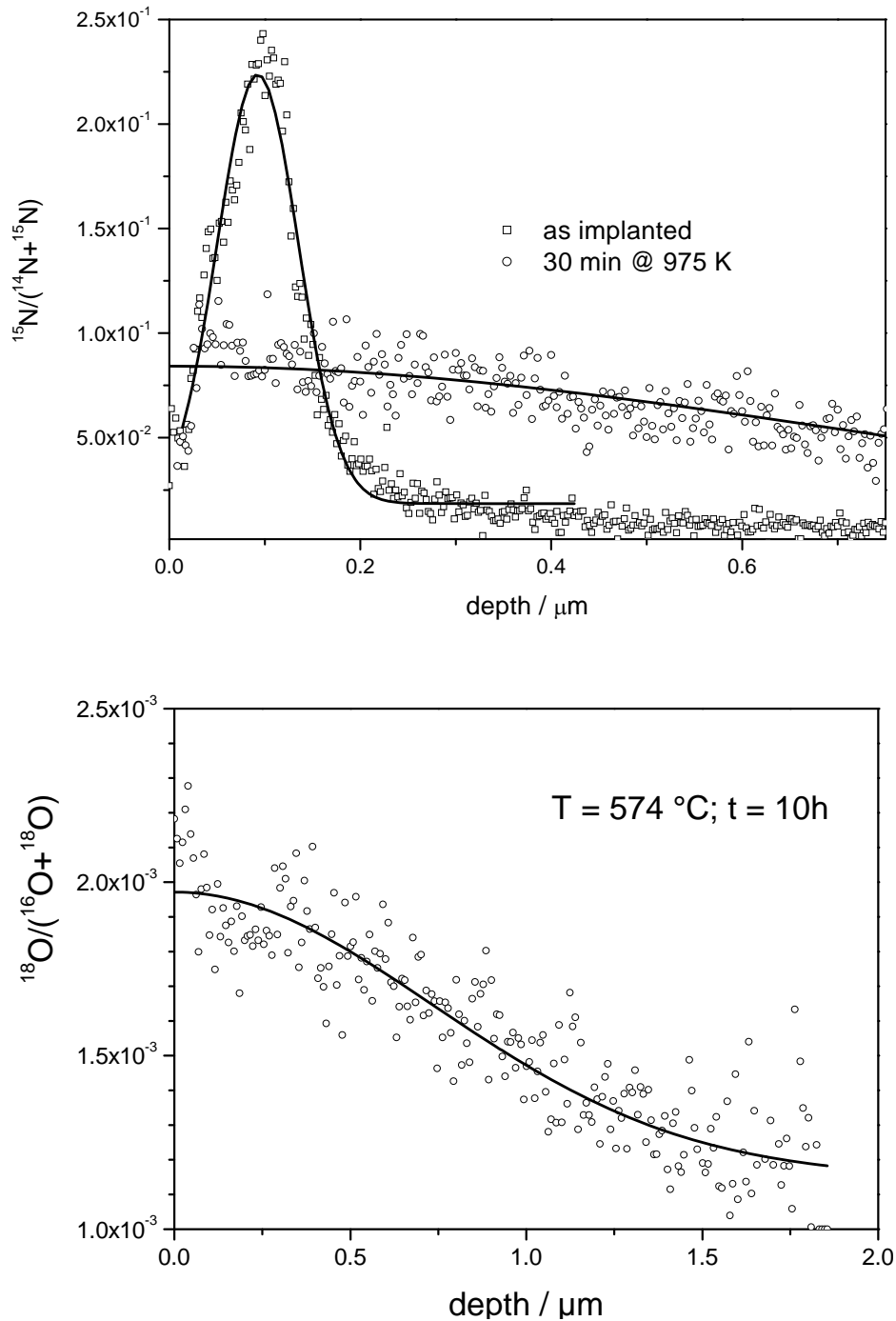


Fig. 1: Nitrogen and Oxygen self-diffusion profile in 'YZrON' containing 1.6 wt-%. Top: Nitrogen self diffusion; Squares: As implanted. Circles: After 30 min diffusion at 10^{-7} mbar, 975 K. Bottom: Oxygen self-diffusion, implanted with ^{18}O and diffused for 10 h at 10^{-7} mbar, 847 K.

Taking $a = 5.14 \text{ \AA}$ being the lattice constant of 'YZrON' [3], $f = 0.65$ being the correlation factor, and $\nu_0 = 1.3 \cdot 10^{13} \text{ s}^{-1}$ being the Debye frequency [18], one gets a value of $5 k_B$. For migration along vacancies, one would expect a value of $3 k_B$; the obtained value of $5 k_B$ is, especially when considering the relatively large experimental error of D_0 , still in agreement with the assumption of a migration along free vacancies. In particular, if there were a migration

along clusters, the activation entropy should be strongly affected. This means that there is no strong evidence for the diffusion of nitrogen through microdomains. The diffusion of nitrogen seems to occur straight along the anion vacancy lattice.

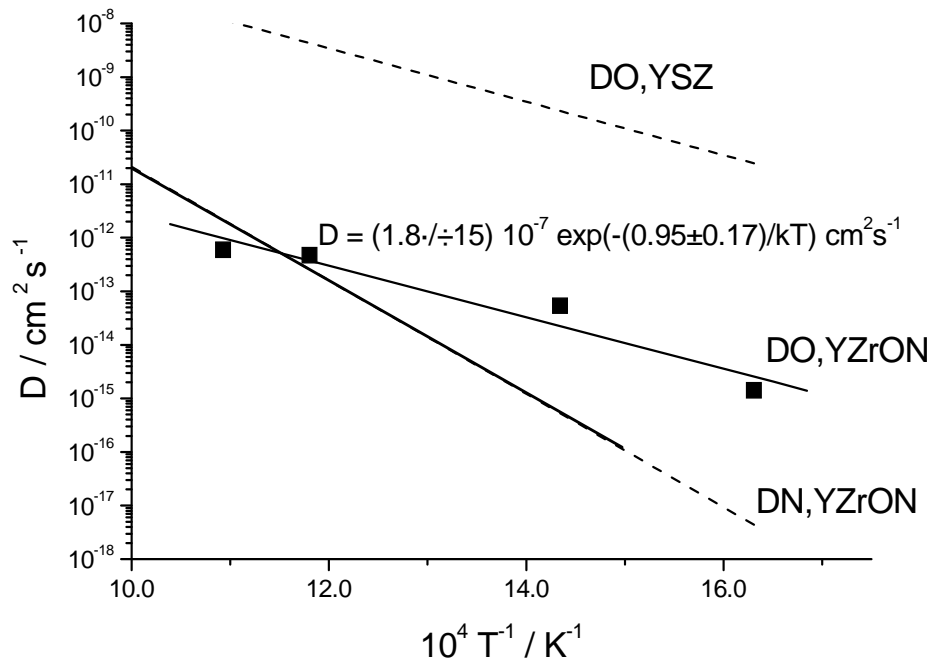


Fig. 2: Arrhenius plot of nitrogen self-diffusion profile in 'YZrON' containing 1.6 wt-% nitrogen.

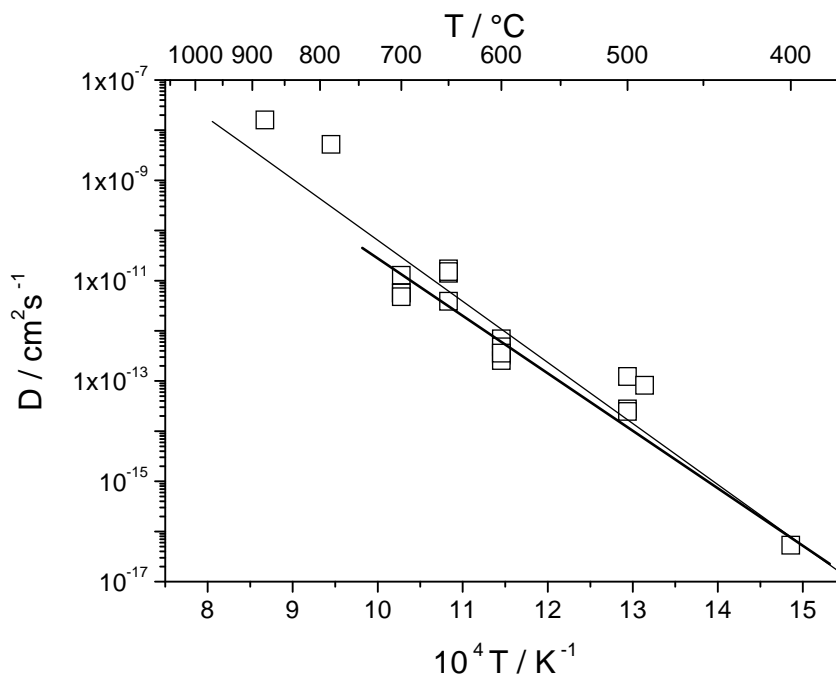


Fig. 3: Oxygen self-diffusion in 'YZrON' containing 1.6 wt-% nitrogen. For comparison, the result of the Arrhenius analysis in Fig. 1 (DN, 'YZrON') and the results of oxygen self-diffusion in YSZ containing the same amount of yttria (DO, YSZ) are included in the plot.

This is different in the case of oxygen diffusion: The very low preexponential factor of the Arrhenius fit corresponds to activation entropy of $-10 k_B$. This value would be indicative for a transport along clusters or strong ordering effects. This is also confirmed by the comparison between the oxygen diffusivity in YSZ and YZrON: The latter is lowered by several orders in magnitude (see Fig. 3) for a system with a comparable number of oxygen vacancies. This means that the doping with nitrogen strongly decelerated the oxygen transport.

3.3 Neutron Diffraction

The effective one particle potential maps (OPPs) [12] as derived from the neutron diffraction experiments are plotted in Fig. 4. Fig. 4a) shows the result for the 'YZrON' containing 2.56 wt% nitrogen ($Zr_{0.96}Y_{0.04}O_{1.64}N_{0.22}$), and Fig. 4b) for the pure cation doped sample. From these plots, it can be seen that the migration proceeds straight along the $\langle 100 \rangle$ directions, the directions of the valley connecting two anion sites. The saddle point corresponds to the potential barrier for migration (1.2 eV for 'YZrON' and 1.09 eV for YSZ). For jumps along $\langle 110 \rangle$ or $\langle 111 \rangle$ directions, the migration barrier is much larger, *i.e.*, such jumps can be excluded at least at not too high temperatures.

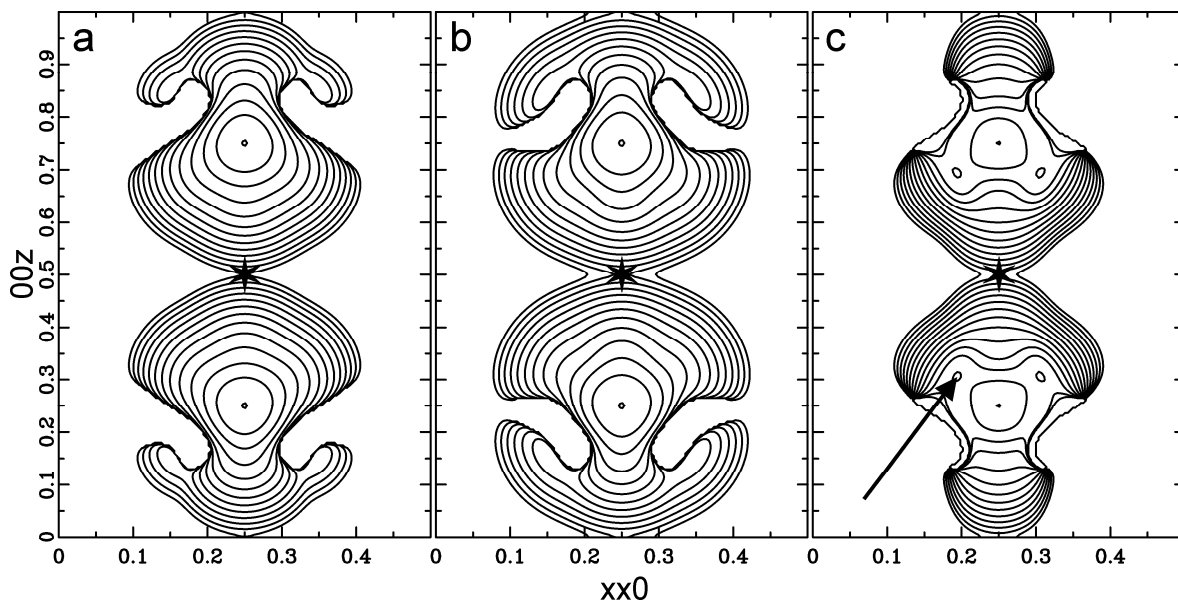


Fig. 4: OPP maps of $Zr_{0.96}Y_{0.04}O_{1.64}N_{0.22}$ (a) and $Zr_{0.74}Y_{0.26}O_{1.87}$ (b). From (a) and (b) the OPP map for nitrogen migration shown in Fig. 4c) was derived. Note the marked side minimum in 4c around $x = 0.16, z = 0.33$ and its corresponding symmetrically equivalent minima.

Although the trajectory straight along the $\langle 100 \rangle$ directions of the fluorite lattice appears to be sterically hindered by the cations (Fig. 5) at first sight, the results found here exclude the possibility of curved pathways through the faces of the cation tetrahedra. This may be understood by taking into account the short range order as determined from previous diffuse scattering studies [13]: There it was found that the anions are displaced from their ideal positions towards the common cation edge, *i.e.*, the actual jump distance is decreased, and these cations are moved apart, *i.e.*, the 'bottle neck' for the jump is opened up [12]. In fact, at high temperatures this scenario has to be regarded as a dynamic process, *i.e.*, the diffusion jumps are assisted by suitable phonons. Assuming statistical independence of the probability densities of oxygen and nitrogen atoms in the *average* structure it is possible (for details see [12]) to separate the contributions due to oxygen and nitrogen migration by comparing the results for two samples with the same amount of vacancies, but with (sample (C), Fig. 4a) and without (*i.e.*

"pure" oxygen, sample (B), Fig. 4b) nitrogen. As a result one gets the OPPs for "pure" nitrogen migration shown in Fig. 4c). Both "pure" OPPs show very similar features with respect to the directions of transport (mainly along $\langle 100 \rangle$, but possibly via metastable positions for nitrogen, see the slight side minima in Fig. 4c), but strongly different activation enthalpies for migration: 1.1 eV for oxygen transport and 2.0 eV for nitrogen transport, respectively. These results are very close to the results of the self-diffusion experiments.

4 Conclusions

Anion transport in 'YZrON' single crystals was investigated by two rather different experimental methods: neutron diffraction and tracer diffusion. The results for the activation enthalpies are in excellent agreement with each other. Nitrogen self-diffusion has almost twice the activation enthalpy of oxygen self-diffusion, about 2 and 1 eV, respectively. At temperatures around 1000 K, nitrogen and oxygen transport coefficients are roughly identical. Neutron diffraction experiments showed furthermore that both nitrogen as well as oxygen transport proceeds mainly along the $\langle 100 \rangle$ directions. The fact that both experiments give similar activation enthalpies means that there is no appreciable enthalpy for the creation of defects, since tracer diffusion includes both, the enthalpies for migration and defect creation, while neutron diffraction measures only that for migration.

Acknowledgement. Ion implantation performed at U Paris-Sud by B. Lesage and O. Kaïtasov is gratefully acknowledged. Financial support of the DFG within SPP1136 is highly acknowledged.

References

- [1] E.H. Kisi (ed.), Zirconia Engineering Ceramics: Old Challenges - New Ideas, Key Engng. Mater. 153/154, Uetikon-Zürich: Trans Tech Publ. 1998.
- [2] S.P.S. Badwal, J. Drennan, Solid State Ionics 53-56 (1992) 769.
- [3] M. Lerch, J. Lerch, K. Lerch, J. Mater. Sci. Lett. 15 (1996) 2127.
- [4] I. Valov, V. Rührup, R. Klein, C. Rödel, M. Dogan, H. D. Wiemhöfer, M. Lerch, J. Janek, Solid State Ionics, submitted
- [5] T.-J. Chung, H. Song, G.-H. Kim, D.-Y. Kim, J. Am. Ceram. Soc. 80 (1997) 2607.
- [6] D.J.M. Bevan, J. Mohyla, K.S. Wallwork, H.J. Rossell, E. Schweda, Z. Anorg. Allg. Chemie 628 (2002) 1180.
- [7] M. Lerch, J. Wrba, J. Lerch, J. Solid State Chem. 125 (1996) 153.
- [8] A.T. Tham, C. Rödel, M. Lerch, D. Wang, D.S. Su, A. Klein-Hoffmann, R. Schlögl, Crystal Research and Technology 39 (2004) 421 and 40 (2005) 193.
- [9] M. Kilo, R.A. Jackson, G. Borchardt, Philos. Mag. 83 (2003) 3309.
- [10] J.-S. Lee, M. Lerch, J. Maier, J. Solid State Chem. 179 (2006) 270.
- [11] M. Kilo, G. Borchardt, B. Lesage, O. Kaïtasov, S. Weber, S. Scherrer, J. Europ. Ceram. Soc. 20 (2000) 2069.
- [12] I. Kaiser-Bischoff, H. Boysen, C. Scherf, T. Hansen, Phys. Chem.-Chem. Phys. 7 (2005) 2061.
- [13] I. Kaiser-Bischoff, H. Boysen, F. Frey, J.-U. Hoffmann, D. Hohlwein, M. Lerch, J. Appl. Cryst. 38 (2005) 139.
- [14] M. Kilo, C. Argirusis, G. Borchardt, R.A. Jackson, Phys. Chem.-Chem. Phys. 5 (2003) 2219.
- [15] J.F. Ziegler, SRIM: The stopping and range of ions in matter, version SRIM 2003, www.srim.org.
- [16] P.S. Manning, J.D. Sirman, R.A. de Souza, J.A. Kilner, Solid State Ionics 100 (1997) 1.
- [17] M. Kilo, M.A. Taylor, C. Argirusis, G. Borchardt, B. Lesage, S. Weber, S. Scherrer, M. Schroeder, M. Martin, J. Appl. Phys. 94 (2003) 7547.
- [18] J.D. Solier, I. Cachadiña, A. Dominguez-Rodriguez, Phys. Rev. B45 (1993) 3704.